

# GAS NEAR A WALL: A SHORTENED MEAN FREE PATH, REDUCED VISCOSITY, AND THE MANIFESTATION OF A TURBULENT KNUDSEN LAYER IN THE NAVIER-STOKES SOLUTION OF A SHEAR FLOW

RAFAIL V. ABRAMOV

**ABSTRACT.** For the gas near a solid planar wall, we propose a scaling formula for the mean free path of a molecule as a function of the distance from the wall, under the assumption of a uniform distribution of the incident directions of the molecular free flight. We subsequently impose the same scaling onto the viscosity of the gas near the wall, and compute the Navier-Stokes solution of the velocity of a shear flow parallel to the wall. This solution exhibits the Knudsen velocity boundary layer in agreement with the corresponding Direct Simulation Monte Carlo computations for argon and nitrogen. We also find that the proposed mean free path and viscosity scaling sets the second derivative of the velocity to infinity at the wall boundary of the flow domain, which suggests that the gas flow is formally turbulent within the Knudsen boundary layer near the wall.

## 1. INTRODUCTION

An accurate description of the Knudsen velocity boundary layer is a long-standing problem in the study of microflows [15, 18]. Guo et al. [9] proposed to scale the viscosity of the gas near a wall proportionally to the corresponding mean free path scaling (as the viscosity is generally proportional to the mean free path of a gas molecule [4]), where the mean free path scaling near the wall was proposed by Stops [16]. In [16], the scaling implied that the distribution of the free flight directions was proportional to the cosine of the angle between the flight direction and the direction of the shortest distance to the wall (called the “cosine law” in [16]). It appears, however, that a uniform distribution of the molecular flight directions was not addressed so far in the given setting.

In the current work we propose a new scaling for the mean free path of a gas molecule near a solid planar wall, which is based on a uniform distribution of the incident molecular flight directions. We start with the probability distribution of the length of the free flight of a molecule constrained by a general solid obstacle, and, for the special case of a solid planar wall, we derive an exact scaling formula for the mean free path as a function of the distance from the wall. The same scaling subsequently applies to the viscosity of the gas, since the viscosity is proportional to the mean free path [4]. We then compute the Navier-Stokes solution of the velocity of the shear flow parallel to the wall, and observe the emergence of the Knudsen boundary layer. We find this boundary layer to be quite similar to the one produced by the Direct Simulation Monte Carlo (DSMC) computations for argon and nitrogen under normal conditions. In comparison,

---

DEPARTMENT OF MATHEMATICS, STATISTICS AND COMPUTER SCIENCE, UNIVERSITY OF ILLINOIS AT CHICAGO, 851 S. MORGAN ST., CHICAGO, IL 60607

*E-mail address:* abramov@uic.edu.

the scaling based on the cosine law from [9, 16] does not appear to model the Knudsen boundary layer with comparable accuracy. Also, a surprising feature of the viscosity scaling we propose is that it requires the second derivative of the gas flow velocity to be infinite at the wall boundary of the flow domain, which, from the perspective of the fluid dynamics, suggests that the Knudsen boundary layer is formally turbulent near the wall boundary.

## 2. THE BEHAVIOR OF THE MEAN FREE PATH NEAR A WALL

First, we consider the situation where a gas molecule flies freely until it collides with another gas molecule (no obstacles are present). We denote the conventional molecular mean free path in the absence of obstacles as  $\lambda_0$ . Assuming that a collision is random and can happen anytime with equal probability, here we model it via a Poisson process, such that the length of the free flight  $r$  until a collision is also a random variable. From the elementary theory of random processes [7] it follows that the probability distribution of time until the next collision decays exponentially with increasing time for a Poisson process model. Observing that the speed of the free flight between collisions is constant, we conclude that the probability distribution function  $f(r)$  of the length  $r$  of the free flight until a collision also decays exponentially with increasing  $r$ :

$$(2.1) \quad f(r) = \frac{1}{\lambda_0} e^{-r/\lambda_0}.$$

The factor in front of the exponent above ensures that  $f(r)$  is normalized; also, the expectation  $\mathbb{E}$  of the length  $r$  of the free flight until a collision is precisely  $\lambda_0$ . The same statistical distribution of the length of the free flight was used in [16] (see the formula at the bottom of p. 686 in [16]), and, for the thermodynamic conditions close to normal, is also corroborated by the direct molecular dynamics simulations in [5] (see Fig. 3(a) in [5]).

Second, let an obstacle be placed along the direction of the flight at the distance  $r_0$  from the current position of the gas molecule, such that the collision is guaranteed to occur before or at  $r_0$ . In this case, the expectation  $\mathbb{E}$  of the length  $r$  of the free flight until a collision (either with another molecule, or, if none happens, with the obstacle upon covering the distance  $r_0$ ) becomes a function of  $r_0$  and is given by

$$(2.2) \quad \mathbb{E}(r_0) = \int_0^{r_0} r f(r) dr + r_0 \int_{r_0}^{\infty} f(r) dr = \lambda_0 \left(1 - e^{-r_0/\lambda_0}\right).$$

Above, the expectation integral is separated into two parts: the first part computes the portion of the expectation of the mean free path for the event where the molecule does not reach the obstacle (by colliding with another molecule); the second part adds the portion corresponding to the complementary event, given by the product of the distance to the obstacle (since that would be the length of the free path for such an event) and the probability of this event.

Third, let the direction of the flight be given by  $\theta$  and  $\phi$ , which are the azimuthal and polar angles, respectively, of a suitable spherical coordinate system. Let us assume that the possible directions of the molecular flight are distributed with the probability

density  $g(\theta, \phi)$ , which satisfies the normalization condition

$$(2.3) \quad \int_0^{2\pi} \int_0^\pi g(\theta, \phi) \sin \phi \, d\phi \, d\theta = 1.$$

Also, let the corresponding distance to the obstacle depend on the direction of the free flight, that is,  $r_0 = r_0(\theta, \phi)$ . Then, in order to compute the mean free path  $\lambda$ , we integrate  $\mathbb{E}(r_0)$  against  $g(\theta, \phi)$  as follows:

$$(2.4) \quad \lambda = \int_0^{2\pi} \int_0^\pi \mathbb{E}(r_0(\theta, \phi)) g(\theta, \phi) \sin \phi \, d\phi \, d\theta = \\ = \lambda_0 \left( 1 - \int_0^{2\pi} \int_0^\pi e^{-r_0(\theta, \phi)/\lambda_0} g(\theta, \phi) \sin \phi \, d\phi \, d\theta \right).$$

Fourth, let a planar wall be placed at the distance  $d$  from the origin along the “north pole” direction of the spherical coordinate system, and let the “southern” hemisphere be free of obstacles. Then,  $r_0(\theta, \phi)$  is given by

$$(2.5) \quad r_0(\theta, \phi) = \begin{cases} d / \cos \phi, & 0 \leq \phi < \pi/2, \\ \infty, & \pi/2 \leq \phi \leq \pi. \end{cases}$$

In this case, the formula in (2.4) becomes

$$(2.6) \quad \lambda = \lambda_0 \left( 1 - \int_0^{2\pi} \int_0^{\pi/2} e^{-d/(\lambda_0 \cos \phi)} g(\theta, \phi) \sin \phi \, d\phi \, d\theta \right).$$

Observe that above in (2.6) the form of the directional probability distribution  $g(\theta, \phi)$  is unimportant for  $\phi > \pi/2$  (that is, for the flight directions escaping the wall). Thus, in what follows, we only need to define  $g(\theta, \phi)$  for the incident flight directions, that is, for  $0 \leq \phi \leq \pi/2$ . Next, we are going to consider two different options for  $g(\theta, \phi)$ : the uniform distribution and the cosine distribution.

**2.1. Uniform distribution of incident flight directions.** Here we assume that

$$(2.7) \quad g_u(\theta, \phi) = \frac{1}{4\pi} \quad \text{for } 0 \leq \phi \leq \pi/2,$$

that is, the distribution of the incident flight directions is uniform. This seems to be a reasonable choice in the absence of a more detailed statistical information on the flight directions in the vicinity of a wall. Observe that the integral of  $g_u$  over the “northern” hemisphere yields  $1/2$ , as, on average, the number of molecules approaching the wall equals the number of molecules escaping the wall.

The assumption of the invariance of  $g$  over the directions (and, in particular, the azimuthal angle) implies that the bulk of the gas is moving uniformly in the chosen coordinate system (in particular, there is no velocity shear). While not strictly true in the numerical experiments which are to follow, we show below via a simple estimate that the effect of the imposed velocity shear on the mean free path scale is minuscule compared to the bulk average molecular speed for normal conditions, and thus cannot substantially invalidate the assumption above.

For the uniform distribution of the flight directions, the integral in (2.6) is evaluated as

$$(2.8) \quad \int_0^{2\pi} \int_0^{\pi/2} e^{-d/(\lambda_0 \cos \phi)} \frac{1}{4\pi} \sin \phi \, d\phi \, d\theta = \frac{1}{2} \left( e^{-d/\lambda_0} - \frac{d}{\lambda_0} E_1(d/\lambda_0) \right),$$

where  $E_1$  is a standard notation for the exponential integral

$$(2.9) \quad E_1(x) = \int_x^\infty \frac{e^{-y}}{y} \, dy.$$

Thus, we find that the mean free path  $\lambda$  at the distance  $d$  away from the wall is given by the following scaling formula:

$$(2.10) \quad \lambda_u(d) = \lambda_0 \left( 1 - \frac{1}{2} \beta_u(d/\lambda_0) \right), \quad \beta_u(x) = e^{-x} - x E_1(x).$$

**2.2. Cosine distribution of incident flight directions.** What is to follow leads to the single-wall variant of the scaling formula suggested by Stops [16] and tested by Guo et al. [9], and thus we present it here for completeness. Here we set

$$(2.11) \quad g_c(\theta, \phi) = \frac{1}{2\pi} \cos \phi \quad \text{for } 0 \leq \phi \leq \pi/2,$$

that is, the probability of the incident flight direction is proportional to the cosine of the angle between the flight direction and the direction of the shortest distance to the wall. Observe that the integral of  $g_c$  over the “northern” hemisphere equals 1/2, for the same reasons as for  $g_u$  above. As for the uniform distribution above, the independence on the azimuthal angle implies that the effect of the velocity shear on the mean free path scale, if present, is small in comparison to the bulk average speed of molecules (which we show to be true for the numerical experiments below).

In this case, the integral in (2.6) is evaluated as

$$(2.12) \quad \int_0^{2\pi} \int_0^{\pi/2} e^{-d/(\lambda_0 \cos \phi)} \frac{1}{2\pi} \cos \phi \sin \phi \, d\phi \, d\theta = \frac{1}{2} \left( \left( 1 - \frac{d}{\lambda_0} \right) e^{-d/\lambda_0} + \left( \frac{d}{\lambda_0} \right)^2 E_1(d/\lambda_0) \right).$$

Thus, we find that the mean free path  $\lambda$  at the distance  $d$  away from the wall is given by the following scaling formula:

$$(2.13) \quad \lambda_c(d) = \lambda_0 \left( 1 - \frac{1}{2} \beta_c(d/\lambda_0) \right), \quad \beta_c(x) = e^{-x} - x \beta_u(x).$$

The formula above is the single-wall version of the scaling that was tested by Guo et al. [9] (see Eq. (3) in [9] with the distance to the second wall set to infinity), which, in turn, was derived by Stops [16] (see, for example, the first formula on p. 689 in [16], and observe that it refers only to a half of the total number of molecules).

**2.3. A comparison between the uniform and cosine scalings.** The difference between the uniform scaling in (2.10) and the cosine scaling in (2.13) is significant; we compare the two scalings visually in Figure 1. Observe that even though both scalings are monotonic concave functions which have the same limits at zero and infinity, their behavior is otherwise different.

The immediately noticeable qualitative difference between the two scalings is the behavior of their derivatives at zero: while the derivative of the uniform scaling in (2.10) at zero is infinite, for the cosine scaling in (2.13) it equals 1. This qualitative difference is important; as we show below, the uniform scaling in (2.10) implies that, from the fluid dynamics perspective, the flow is formally turbulent near the wall boundary of the flow domain, whereas in the case of the cosine scaling in (2.13) the second derivative of the velocity remains finite at the wall boundary.

Quantitatively, the relative difference between the two scalings reaches 9% at the distance of roughly 20% of the conventional mean free path  $\lambda_0$  away from the wall. It is also interesting that the uniform scaling (2.10) in Figure 1 visually looks similar to the data computed from the direct molecular dynamics simulations in [5] (see Fig. 4 in [5]).

### 3. AN EXPLICIT NAVIER-STOKES SOLUTION FOR THE SHEAR FLOW NEAR A WALL

According to the kinetic theory of gases [4], the viscosity  $\mu$  is proportional to the free mean path of a gas molecule. Therefore, the uniform and cosine scalings for the mean free path in (2.10) and (2.13), respectively, imply that the viscosity scales in the same manner:

$$(3.1) \quad \mu(d) = \mu_0 \left( 1 - \frac{1}{2} \beta(d/\lambda_0) \right),$$

where  $\mu_0$  is the conventional value of the viscosity (computed as if no wall was present) for the given gas parameters, and  $\beta$  is either the uniform scaling  $\beta_u$  from (2.10), or the cosine scaling  $\beta_c$  from (2.13). The same proposition was made in [9].

The transport equation for the velocity  $\mathbf{u}$  is given by

$$(3.2) \quad \frac{\partial(\rho \mathbf{u})}{\partial t} + \operatorname{div}(\rho \mathbf{u} \mathbf{u}^T + p \mathbf{I} + \mathbf{S}) = 0,$$

where  $\rho$  is the density,  $p$  is the pressure, and  $\mathbf{S}$  is the stress tensor. The transport equation for the stress tensor  $\mathbf{S}$  with the linearized collision term is, in turn, given by [1, 8, 13]

$$(3.3) \quad \frac{\partial \mathbf{S}}{\partial t} + \operatorname{div}(\mathbf{u} \otimes \mathbf{S} + \mathbf{Q}) + \mathbf{P} \nabla \mathbf{u} + (\mathbf{P} \nabla \mathbf{u})^T + (1 - \gamma)(\operatorname{tr}(\mathbf{P} \nabla \mathbf{u}) + \operatorname{div} \mathbf{q}) \mathbf{I} = -\frac{p}{\mu} \mathbf{S},$$

where  $\mathbf{P} = p \mathbf{I} + \mathbf{S}$  is the pressure tensor,  $\mathbf{q}$  is the heat flux,  $\mathbf{Q}$  is the full centered third moment (a tensor of rank 3), and  $\gamma$  is the adiabatic exponent. Then, the Navier-Stokes approximation for  $\mathbf{S}$  is obtained under the assumption that all terms in the left-hand side of (3.3), except for those which involve  $p$  and  $\mathbf{u}$  only, are small and can be discarded. This leads to the approximation

$$(3.4) \quad \mathbf{S} = -\mu \left( \nabla \mathbf{u} + (\nabla \mathbf{u})^T + (1 - \gamma)(\operatorname{div} \mathbf{u}) \mathbf{I} \right),$$

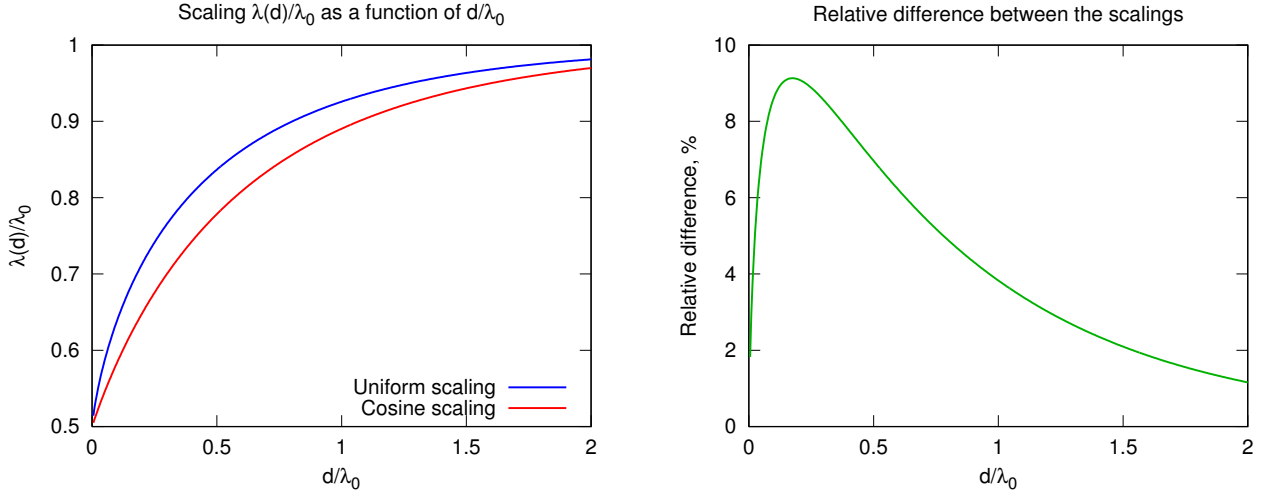


FIGURE 1. A visual comparison of the uniform (2.10) and cosine (2.13) mean free path scalings.

which is then substituted into the velocity transport equation (3.2) to obtain the usual Navier-Stokes equation.

For a stationary shear flow, let us choose a coordinate system where the  $x$ -coordinate points in the direction of the flow, and the  $y$ -coordinate points in the direction of the shear. In this situation, the velocity vector  $\mathbf{u}$  points along the  $x$ -direction, but the spatial dependence of the flow variables occurs in the  $y$ -direction. As the  $y$ -coordinate measures the distance to the wall, we will use  $d$  to denote the  $y$ -coordinate:

$$(3.5) \quad \mathbf{u} = (u(d), 0, 0)^T, \quad \text{div} \mathbf{S} = ((\mu u)')^T, 0, 0)^T,$$

where the prime denotes the  $d$ -differentiation. This form of the velocity yields, upon the substitution of the Navier-Stokes approximation to  $\text{div} \mathbf{S}$  above in (3.4) back into the stationary velocity equation (3.2),

$$(3.6) \quad (\mu u)' = 0.$$

**3.1. The velocity solution for the boundary value problem of the shear flow.** For convenience, we set the flow velocity  $u$  to zero at the wall boundary of the flow domain, and to  $u_0$  at the distance  $d_0$  from the boundary. Observe that in reality the gas flow velocity exhibits a discontinuous “slip” directly at the wall surface [11, 12], that is, the velocity of the gas flow at the wall is not that of the wall itself. This kinetic effect, however, is beyond the scope of the current work, as, from the perspective of the fluid dynamics, we consider a spatial domain with suitable boundaries (which do not have to be aligned with walls in general, as the domain may simply be a bounded “cutout” of the free gas flow away from any walls or other objects), and it is the properties of the gas flow itself which are defined at the boundaries, irrespective of whether or not a wall is present immediately outside the boundary. Thus, in what follows, we refer strictly to the velocity of the gas flow at a wall boundary, regardless of the (possibly different) velocity of the wall itself.

We further assume that the temperature of the gas flow varies insignificantly, so that the conventional viscosity  $\mu_0$  in (3.1) (computed as if no wall was present) can be treated as a constant. Then, for a constant viscosity  $\mu$  without the mean free path scaling, the Navier-Stokes equation for the velocity of the shear flow in (3.6) reduces to

$$(3.7) \quad u'' = 0,$$

which leads to the conventional linear shear velocity profile solution

$$(3.8) \quad u(d) = u_0 \frac{d}{d_0}.$$

On the other hand, with the variable viscosity in (3.1), the Navier-Stokes velocity equation (3.6) for the shear flow becomes

$$(3.9) \quad \left( \left( 1 - \frac{1}{2} \beta(d/\lambda_0) \right) u(d)' \right)' = 0.$$

Upon the integration with the same boundary conditions as above, (3.9) results in

$$(3.10) \quad u(d) = u_0 \frac{b(d/\lambda_0)}{b(d_0/\lambda_0)}, \quad b(x) = \int_0^x \frac{dy}{2 - \beta(y)},$$

where  $\beta$  is given by either the uniform scaling in (2.10), or the cosine scaling in (2.13).

**3.2. Wall boundary turbulence in the case of the uniform viscosity scaling.** Observe that, in the case of the uniform viscosity scaling (that is,  $\beta = \beta_u$  from (2.10)) the identity above in (3.9) requires the second derivative  $u''(d)$  to become infinite at the wall boundary. Indeed, substituting (2.10) into (3.9), we obtain

$$(3.11) \quad u(d)'' = \frac{u(d)'}{2\lambda_0} \left( 1 - \frac{1}{2} \beta_u(d/\lambda_0) \right)^{-1} \beta_u'(d/\lambda_0).$$

However, observe that

$$(3.12) \quad \beta_u'(x) = (e^{-x} - xE_1(x))' = -E_1(x),$$

and that  $E_1(0)$  is infinite. Thus,  $u''(0)$  must also become infinite for (3.9) to hold. Observe that this condition does not violate the assumptions made above on the stress equation (3.3), as the latter does not involve the second derivatives of the velocity, and the Navier-Stokes approximation of the stress is still valid. In contrast, the cosine mean free path scaling in (2.13) does not have this property.

Recall that sufficiently large second derivatives of the velocity  $u$  cause the viscous term in the Navier-Stokes velocity equation in (3.2) to become of a comparable order in magnitude to the transport terms (as under normal conditions the viscous term is usually small due to low viscosity), which is what is observed in a turbulent flow. In fact, based on this observation, Boussinesq [3] proposed to model the effect of the large second derivatives of the velocity in a turbulent flow with the “eddy viscosity”, that is, an artificially large viscosity coefficient to compensate for the unresolved turbulent fine-grained motion of the flow and to achieve a similar net effect of the stress divergence. The same principle is used in various numerical models of turbulent flow [17]. Thus,

from the fluid dynamics perspective, the infinite second derivative of the velocity at the wall boundary formally makes the boundary layer of the flow turbulent.

Observe, however, that in the current setting the turbulence in the boundary layer is the result of the imposed condition that the viscous term in the velocity equation (3.2) is bounded near the wall, which is directly opposite to the effect of the turbulence away from the wall. Nonetheless, this effect suggests that the uniform mean free path scaling in (2.10) may hint at the actual physical mechanism of the turbulence manifestation in a shear flow – for example, when some appropriate instability conditions are satisfied, the turbulence near the wall boundary may “spill” into the flow outside the boundary layer.

#### 4. NUMERICAL EXPERIMENTS

Here we compare the gas flow velocity profiles corresponding to the uniform mean free path scaling in (2.10) and the cosine scaling in (2.13) with the Direct Simulation Monte Carlo computations (DSMC) for argon and nitrogen. For a better reliability of the DSMC computations results, we used two different publicly available DSMC software codes: one is the DS1V [2]<sup>1</sup>, and another is the dsmcFoam [14]<sup>2</sup>. For both argon and nitrogen, the temperature and pressure were set at about 15° C and 100 kPa respectively, which correspond to the normal conditions at sea level. The shear in the flow was imposed by placing two infinite parallel moving walls (the so-called Couette flow) with diffuse reflection boundary conditions at the distance of 1000 nanometers from each other. The relative difference in the wall velocity was 100 meters per second. Due to the symmetry of the flow, below we consider only a half of the flow domain, between one of the walls and the middle point between the walls (such that the width of our domain is 500 nm).

For convenience, we removed the wall slip from the DSMC velocity profile by subtracting its zero-distance value. This also resulted in the DSMC velocity at 500 nm away from the wall being about 45 m/s (rather than half of the wall velocity difference, that is, 50 m/s). As explained above, we did not consider the wall itself to be a part of the domain, and thus chose the coordinate system so that the DSMC flow velocity was zero at the wall boundary of the domain.

The observed temperature variation in the DSMC solutions was about two degrees, which corresponds to the variation of about 0.3% in the conventional value of the viscosity  $\mu_0$  across the flow domain. The effect of the velocity shear in the DSMC simulation on the assumed uniformity of free flight directions is also small: indeed, observe that the change of 45 m/s on the 500 nm scale translates to about 6 m/s on the 60-70 nm (mean free path) scale. At the same time, average speeds of molecules at the room temperature range from about 400 (argon) to about 500 (nitrogen) m/s, so that the velocity shear effect accounts for no more than 1.5% of the typical molecular velocity on the mean free path scale.

In Figures 2 and 3 we compare the constant-viscosity linear solution in (3.8) and the nonlinear solutions in (3.10) corresponding to the uniform mean free path scaling

<sup>1</sup>Available at <http://www.gab.com.au>

<sup>2</sup>Part of the OpenFOAM software, <http://www.openfoam.org>

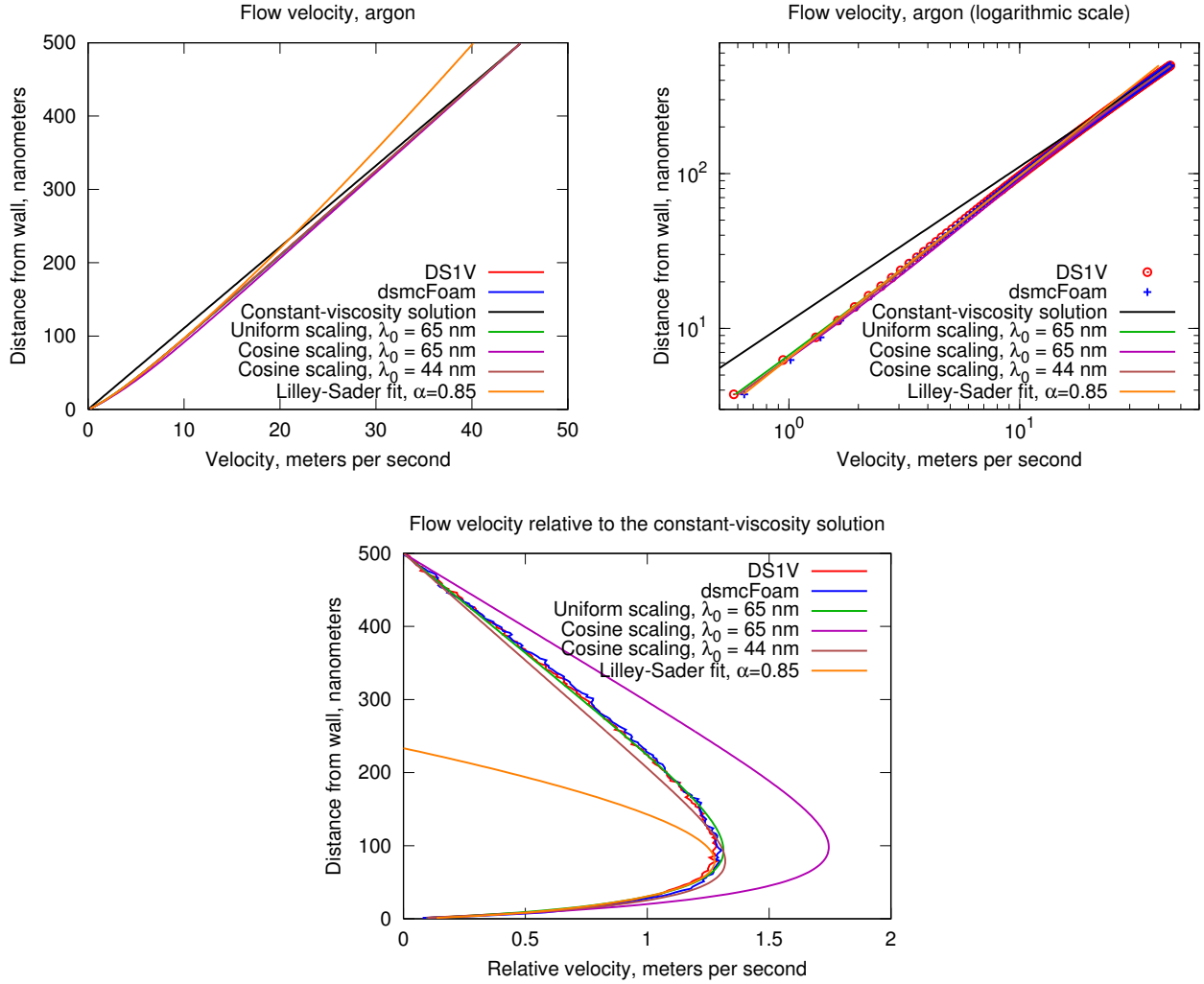


FIGURE 2. The velocity of the shear flow for argon.

in (2.10) and cosine scaling (2.13) for argon and nitrogen with the corresponding velocity profiles computed by the DS1V [2] and dsmcFoam [14] software as described above. We used the DSMC-computed velocity values at 500 nm as the boundary conditions  $u_0$  in (3.8) and (3.10). We set the conventional mean free path  $\lambda_0$ , which is a parameter in (3.10), to 65 nanometers for argon (Figure 2) and to 60 nanometers for nitrogen (Figure 3), which appear to be realistic enough for the normal conditions [10]. Observe that the range of the flow domain (from zero to 500 nm) extends well beyond the Knudsen boundary layer region.

For illustrative purposes, we also show the velocity power fit of Lilley and Sader [11,12] of the form

$$(4.1) \quad u(d) = C(d/\lambda_0)^\alpha,$$

where the constant  $\alpha$  was computed by the least squares fit on the DSMC velocity data between the wall and  $\lambda_0$  (for both argon and nitrogen, the least squares algorithm

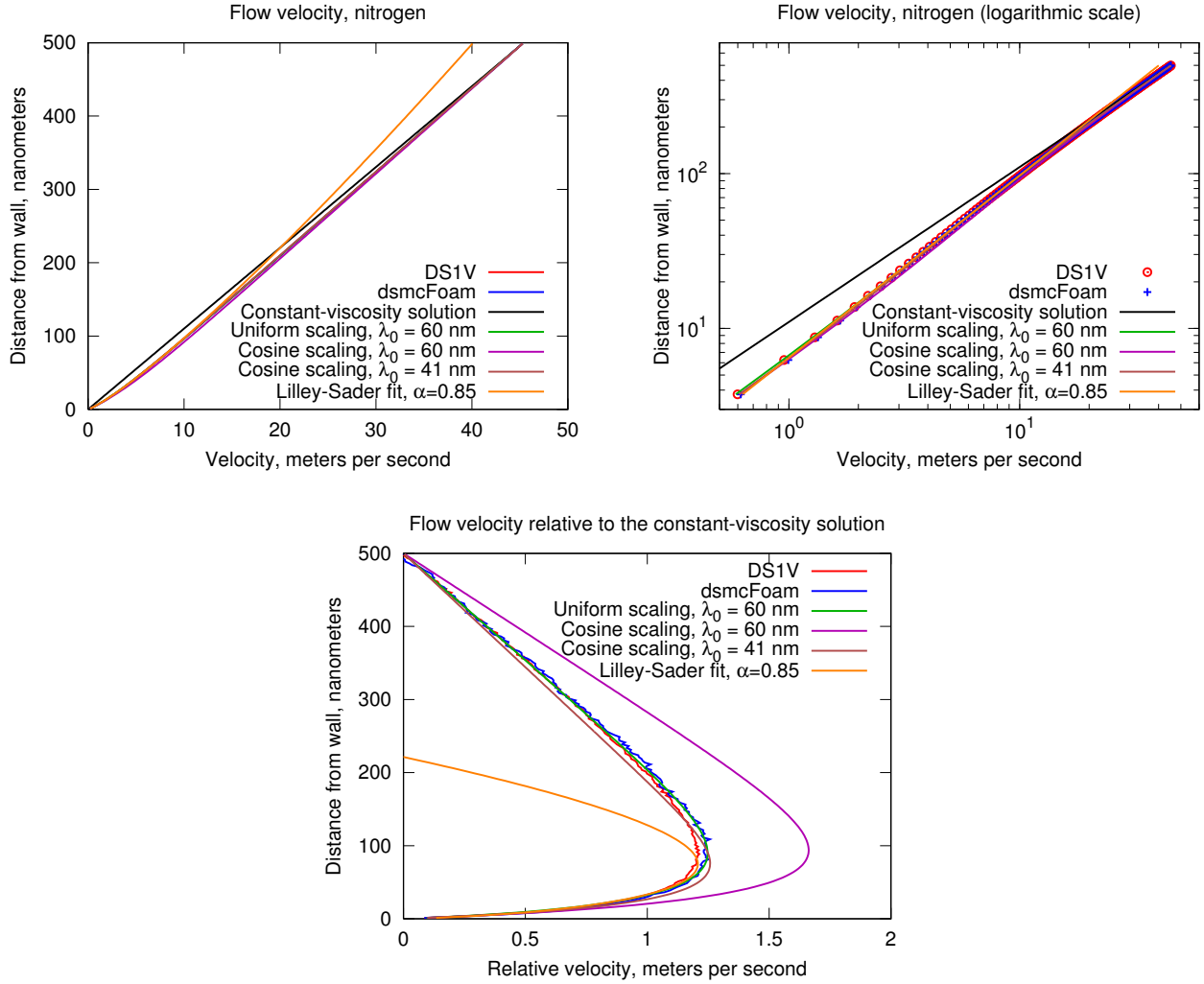


FIGURE 3. The velocity of the shear flow for nitrogen.

yielded  $\alpha = 0.85$ ). The constant coefficient  $C$  was set to the average value of DS1V and dsmcFoam flow velocities at the distance of the conventional mean free path  $\lambda_0$  from the wall.

Observe that the Knudsen boundary layers, produced by the DSMC simulations, are captured quite accurately by the velocity solution in (3.10) with the uniform mean free path scaling in (2.10) for both argon and nitrogen. In contrast, the conventional constant-viscosity Navier-Stokes solution (3.8) fails to develop a boundary layer at all, while the solution for the cosine scaling in (2.13) develops a noticeably stronger Knudsen layer than those produced by the DSMC methods. The Lilley-Sader velocity power fit (4.1) is accurate within the Knudsen boundary layer range (which is where it was fitted), but quickly diverges from the DSMC solutions outside the Knudsen boundary layer.

Additionally, we computed the velocity profiles using the cosine scaling in (2.13) with the mean free path parameter  $\lambda_0$  artificially chosen so as to match the resulting velocity profile to the DSMC results as close as possible (44 nm for argon, and 41 nm for nitrogen).

Argon		Nitrogen	
Scaling	Relative error	Scaling	Relative error
Uniform, $\lambda_0 = 65$ nm	$7.564 \cdot 10^{-4}$	Uniform, $\lambda_0 = 60$ nm	$5.399 \cdot 10^{-4}$
Cosine, $\lambda_0 = 65$ nm	$1.1 \cdot 10^{-2}$	Cosine, $\lambda_0 = 60$ nm	$1.059 \cdot 10^{-2}$
Cosine, $\lambda_0 = 44$ nm	$1.822 \cdot 10^{-3}$	Cosine, $\lambda_0 = 41$ nm	$1.444 \cdot 10^{-3}$

TABLE 1. Relative errors for different scalings.

The results are also shown in Figures 2 and 3. Observe that, even given the unrealistic values of  $\lambda_0$  for an artificially better fit, the resulting velocity profiles are still not as accurate as the ones produced by the uniform scaling in (2.10) with realistic values of  $\lambda_0$ .

We summarize the computational results in Table 1, which contains relative errors (in the sense of the usual Euclidean square norm) between the averaged DSMC velocity profile and different scaling approximations in the full flow domain between the wall boundary and 500 nm distance away from the wall. Observe that the uniform scaling in (2.10) offers better accuracy than the cosine scaling in (2.13).

## 5. CONCLUDING REMARKS

In the current work we propose a new mean free path (and, subsequently, viscosity) scaling near a wall based on the uniform distribution of the molecular free flight directions incident on the wall. We also derive the corresponding velocity solution to the conventional Navier-Stokes equation for the shear flow near a wall, based on the proposed scaling. We compare the proposed uniform scaling with the scaling based on the cosine distribution of the incident flight directions suggested by Stops [16] and tested by Guo et al. [9], as well as the Lilley-Sader velocity power fit [11, 12] for the shear flow of argon and nitrogen at normal conditions. The Direct Simulation Monte Carlo computations of two different software codes, DS1V [2] and dsmcFoam [14] are used for the validation of the results. The proposed uniform scaling is found to be more accurate than the other studied approximations in the domain of the simulated flow, which extends well beyond the Knudsen boundary layer.

The proposed viscosity scaling also appears to be convenient for the computational fluid dynamics modeling, since it can be readily integrated into the existing models of a viscous gas flow, provided that the value of the conventional mean free path  $\lambda_0$  can be reliably estimated from the macroscopic parameters of the gas dynamics. Suitable approximate formulas for the exponential integral (which is a part of the mean free path and viscosity scaling formula), can be found in [6].

An unexpected finding of this work is the inherent presence of turbulence, in the formal fluid dynamics sense, within the Knudsen boundary layer near the wall for the uniform viscosity scaling. It is interesting that this result is purely analytic; clearly, the DSMC simulations or experimental measurements cannot detect it. This result could potentially provide some hints at the physical mechanism behind the visible manifestation of turbulence outside the boundary layer – indeed, if the turbulence covertly exists within the Knudsen boundary layer, then it could be a matter of suitable conditions

for it to spread from the boundary layer into the outside flow. Obviously, this finding necessitates a further study.

**Acknowledgment.** The work was supported by the Office of Naval Research grant N00014-15-1-2036.

#### REFERENCES

- [1] R.V. Abramov. Diffusive Boltzmann equation, its fluid dynamics, Couette flow and Knudsen layers. Preprint, 2017.
- [2] G.A. Bird. *Molecular Gas Dynamics and the Direct Simulation of Gas Flows*. Clarendon, Oxford, 1994.
- [3] J. Boussinesq. Essai sur la théorie des eaux courantes. *Mémoires présentés par divers savants à l'Académie des Sciences*, XXIII(1):1–680, 1877.
- [4] S. Chapman and T.G. Cowling. *The Mathematical Theory of Non-Uniform Gases*. Cambridge Mathematical Library. Cambridge University Press, 3rd edition, 1991.
- [5] N. Dongari, Y. Zhang, and J.M. Reese. Molecular free path distribution in rarefied gases. *J. Phys. D: Appl. Phys.*, 44:125502, 2011.
- [6] P.H. Giao. Revisit of well function approximation and an easy graphical curve matching technique for Theis' solution. *Ground Water*, 41(3):387–390, 2003.
- [7] I.I. Gikhman and A.V. Skorokhod. *Introduction to the Theory of Random Processes*. Courier Dover Publications, 1969.
- [8] H. Grad. On the kinetic theory of rarefied gases. *Comm. Pure. Appl. Math.*, 2(4):331–407, 1949.
- [9] Z.L. Guo, B.C. Shi, and C.G. Zheng. An extended Navier-Stokes formulation for gas flows in the Knudsen layer near a wall. *Europhys. Lett.*, 80:24001, 2007.
- [10] J.O. Hirschfelder, C.F. Curtiss, and R.B. Bird. *The Molecular Theory of Gases and Liquids*. Wiley, 1964.
- [11] C.R. Lilley and J.E. Sader. Velocity gradient singularity and structure of the velocity profile in the Knudsen layer according to the Boltzmann equation. *Phys. Rev. E*, 76:026315, 2007.
- [12] C.R. Lilley and J.E. Sader. Velocity profile in the Knudsen layer according to the Boltzmann equation. *Proc. R. Soc. A*, 464:2015–2035, 2008.
- [13] F. Mallinger. Generalization of the Grad theory to polyatomic gases. Research Report 3581, Institut National de Recherche en Informatique et en Automatique, 1998. E-print: INRIA-00073100.
- [14] T.J. Scanlon, E. Roohi, C. White, M. Darbandi, and J.M. Reese. An open source, parallel DSMC code for rarefied gas flows in arbitrary geometries. *Comput. Fluids*, 39(10):2078–2089, 2010.
- [15] Y. Sone. *Kinetic Theory and Fluid Dynamics*. Modeling and Simulation in Science, Engineering and Technology. Springer Science, 2002.
- [16] D.W. Stops. The mean free path of gas molecules in the transition regime. *J. Phys. D: Appl. Phys.*, 3:685–696, 1970.
- [17] D.C. Wilcox. *Turbulence modeling for CFD*. DCW Industries, second edition, 1998.
- [18] W.-M. Zhang, G. Meng, and X. Wei. A review on slip models for gas microflows. *Microfluid. Nanofluid.*, 13:845–882, 2012.